Soft Matter

PAPER

View Article Online
View Journal | View Issue

Cite this: Soft Matter, 2015, 11, 6492

Adhesive loose packings of small dry particles†

Wenwei Liu,[ab] Shuiqing Li,*[a] Adrian Baule[c] and Hernán A. Makse*[b]

Received 14th May 2015,
Accepted 7th July 2015

DOI: 10.1039/c5sm01169h

www.rsc.org/softmatter

We explore adhesive loose packings of small dry spherical particles of micrometer size using 3D discrete-element simulations with adhesive contact mechanics and statistical ensemble theory. A dimensionless adhesion parameter (Ad) successfully combines the effects of particle velocities, sizes and the work of adhesion, identifying a universal regime of adhesive packings for Ad $>$ 1. The structural properties of the packings in this regime are well described by an ensemble approach based on a coarse-grained volume function that includes the correlation between bulk and contact spheres. Our theoretical and numerical results predict: (i) an equation of state for adhesive loose packings that appear as a continuation from the frictionless random close packing (RCP) point in the jamming phase diagram and (ii) the existence of an asymptotic adhesive loose packing point at a coordination number $Z = 2$ and a packing fraction $\phi = 1/2^3$. Our results highlight that adhesion leads to a universal packing regime at packing fractions much smaller than the random loose packing (RLP), which can be described within a statistical mechanical framework. We present a general phase diagram of jammed matter comprising frictionless, frictional, adhesive as well as non-spherical particles, providing a classification of packings in terms of their continuation from the spherical frictionless RCP.

1 Introduction

Packings of particles have been studied to understand the microstructure and bulk properties of liquids, glasses and crystals, as well as granular matter.[1–4] Studies have focused on high density jammed packings, which, in the case of uniform frictionless spheres, are found at the so-called random close packing (RCP) density.[1–6] Mean-field models of metastable glasses under replica symmetry breaking (RSB) have shown that jamming of frictionless hard spheres should intrinsically occur over a range of volume fractions (J-line) $\phi \in [\phi_{th},\phi_{GCP}]$ and at an isostatic coordination number.[2,7–9] Statistical mechanical approaches based on the volume function, first introduced by Edwards,[10] at a mean field level[6,11,12] consider an ensemble average over all mechanically stable configurations at a given coordination number, which average over the J-line packings at a constant coordination number and estimates the jamming fraction ϕ_{Edw} close to the most probable value at the lower boundary of the J-line. In this paper, we work under the mean-field Edwards ensemble approximation which can be easily generalized from spherical frictionless particles to particles of different shapes, friction and adhesive properties. We consider an ensemble average over a fixed coordination number and effectively redrawing the J-line to a single point close to the lower density predicted by mean field replica breaking theory.[2,7–9] Indeed such an approximation provides results consistent with the lower bound of replica theory in infinite dimensional packings.[13]

In the presence of friction, packings reach lower volume fractions up to the random loose packing (RLP) limit $\phi_{RLP} \approx 0.55$.[6,14–16] Frictional packings at densities smaller than ϕ_{RLP} are usually not mechanically stable.[16–19] However, most packings of dry small micrometer-sized particles in Nature are subject to not only friction, but also adhesion forces. In fact, van der Waals forces generally dominate interactions between particles with diameters of around 10 μm or smaller. In this case, the adhesive forces begin to overcome the gravitational and elastic contact forces acting on the particles and change the macroscopic structural properties.[20,21] Despite the ubiquity of adhesive particle packings in almost all areas of engineering, biology, agriculture and physical sciences,[21–24] there have only been few systematic investigations of these packings.[25–30] Previous studies using a discrete element method (DEM) have found that the packing fraction decreases for adhesive microparticles in a range of $\phi = 0.165$–0.622 with smaller sizes,[25] which is also proved within $\phi \approx 0.2$–0.55 for 4–52 μm particles in both simulation and experiment.[30] A random ballistic deposition and a fluidized bed technique was used, respectively, to produce the packing fractions

[a] Key Laboratory for Thermal Science and Power Engineering of Ministry of Education, Department of Thermal Engineering, Tsinghua University, Beijing 100084, China. E-mail: lishuiqing@tsinghua.edu.cn
[b] Levich Institute and Physics Department, City College of New York, New York 10031, USA. E-mail: hmakse@lev.ccny.cuny.edu
[c] School of Mathematical Sciences, Queen Mary University of London, Mile End Road, London E1 4NS, UK

† Electronic supplementary information (ESI) available: Details on the simulation techniques used in the paper. See DOI: 10.1039/c5sm01169h

ϕ = 0.15–0.33 for both uncompressed and compressed samples[27] and ϕ = 0.23–0.41 for samples with particle diameters of 7.8–19.1 μm.[26] The generation of low density aggregates due to attractive interparticle forces is well understood in the case of Brownian colloidal suspensions undergoing gelation.[31–33] Here, arrest at low densities typically arises due to an interrupted liquid-gas phase separation.[34–37]

In this paper, we investigate the low density regime of soft-sphere, non-Brownian, adhesive particles using a discrete element method (DEM). The main challenge in simulations is to single out the effect of the adhesion forces alone, since adhesion, elastic contact forces and friction all couple within the short-range particle–particle interaction zone and are further coupled with fluid forces (*e.g.*, buoyancy, drag and lubrication) across long-range scales. In our method, the fluid effect is filtered out by assuming the gravitational sediment under vacuum conditions. Most importantly, the gravitational effect can be neglected when the relative deviation of the particle velocity due to gravitational acceleration during the deposition process is small: $(U - U_0)/U_0 \ll 1$. Here, $U = \sqrt{(U_0)^2+2gH}$, where H is the characteristic height of the deposition control volume and U_0 the initial particle velocity at the upper inlet boundary. For all runs in the numerical simulations, we ensure that the relative velocity deviation is less than 4%. Therefore, the adhesive packings simply arise due to the competition between the particle inertia and particle–particle interactions (*e.g.*, adhesion, elasticity and friction).

2 Discrete element method simulation

In a novel DEM framework specifically developed for adhesive grains,[20,21] both the transitional and rotational motions of each particle in the system are considered on the basis of Newton's second law (see ESI,† Section I). The adhesive contact forces F_A include three terms, the normal adhesive contact force F_{ne}, the normal damping force F_{nd} validated by classic particle-surface impact experiments,[20,21] and the tangential force due to the sliding friction. A JKR (Johnson–Kendall–Roberts) model is employed to account for F_{ne} between the relatively compliant micro-particles,[38] implying that the length scale of elastic deformation is large compared to the length scale of the adhesive force (with the particles' Tabor parameter larger than unity).[21] The dissipation terms, including the sliding, twisting and rolling frictions in the presence of adhesion, are all approximated by a linear spring–dashpot–slider model with model parameters given in ref. 39. The slider considerations mean that the sliding, twisting and rolling resistances all reach critical values, $F_{s,crit}$, $M_{t,crit}$ and $M_{r,crit}$, as three related displacements exceed certain limits. For displacements larger than those limits, the resistances stay constant and the particles start to slide or spin. The critical limits in the presence of adhesion are given in the following equations,[21,22,40]

$$F_{s,crit} = \mu_f|F_{ne} + 2F_C| \quad (1)$$

$$M_{t,crit} = 3\pi a F_{s,crit}/16 \quad (2)$$

$$M_{r,crit} = -4F_C(a/a_0)^{3/2}\Theta_{crit}R, \quad (3)$$

where μ_f is the friction coefficient, Θ_{crit} is the critical angle for the relative rolling of two particles, and F_C is the critical pull-off force expressed by the work of adhesion (twice the surface energy, $w = 2\gamma$): $F_C = 1.5\pi wR$. Here, R is the effective radius between two contacting particles ($1/R = 1/r_{p_1} + 1/r_{p_2}$) and a is the radius of the contact area with a_0 at equilibrium in the JKR model. The values or ranges of μ_f, Θ_{crit} and F_C are selected according to the data from atomic force microscopy measurements.[40]

The adhesive DEM simulation starts with the random free falling of 1000 spheres with an initial velocity U_0 at a height H (ESI,† Section II).[6,41,42] The horizontal plane for particle deposition has two equal edges of length L, with periodic boundary conditions along the two horizontal directions. Here we focus on uniformly sized particles, with the particle radius ranging from r_p = 1 to 50 μm. A sensitivity analysis shows that the difference in ϕ_{RLP} between the cases $L = 20r_p$ and $L = 40r_p$ is negligible, indicating that $L = 20r_p$ is large enough to reproduce bulk properties (see ESI,† Section II). Then, we set $L = 20r_p$. The work of adhesion (twice the surface energy, $w = 2\gamma$), *e.g.*, for silica microspheres is reported at 20–30 mJ m^{-2}.[21,40] Setting w = 30 mJ m^{-2}, the simulations indicate that both particle deposition velocities and particle sizes significantly affect the packing structures. As shown in Fig. 1 (or more details in Fig. S3, ESI†), either a large velocity or large size can produce a relatively dense packing when other parameters are fixed. A dimensionless adhesion parameter $Ad = w/(2\rho_p U_0^2 R)$, defined as the ratio between interparticle adhesion and particle inertia,[43] can be used to quantify the combined effect of velocity and size. Here, ρ_p is the mass density of particles. Fig. 2 shows the variation of the packing volume fraction as a function of Ad for packings with r_p = 1, 5, 10, and 50 μm with w ranging from 5–30 mJ m^{-2}. In the case of $Ad < 1$, the data points are scattered between RLP and RCP, since particle inertia dominates the adhesion and the friction. However, when $Ad > 1$, we obtain an adhesion-controlled regime, in which the volume fraction decreases exponentially with increasing Ad, becoming linear at large values $Ad \sim 10$. The lowest packing density achieved is ϕ = 0.154 when Ad is as high as 48, which agrees well with the data from a random ballistic deposition experiment[27] and DEM simulations.[25,30] As discussed above, the negligible gravitational effect distinguishes our system from that reported in ref. 25 and 30.

In addition to ϕ, a reproducible observable of the packing is the average coordination number Z, which denotes the average number of contacts of a sphere in the packing. The isostatic conjecture predicts the upper and lower bounds of $Z = 2d$ and $Z = d + 1$ for frictionless and infinitely rough hard-spheres, respectively, in d = 3 spatial dimension. In Fig. 2 (inset), we can see that for $Ad < 1$ the packings lie indeed within the isostatic limits reaching the infinitely rough value of Z = 4 at $Ad \approx 1$. This indicates that weak adhesion has a similar effect on the packing as strong friction. For $Ad > 1$, the adhesive packings fall on a unique curve, analogous to the ϕ dependence. The lowest Z reached in our simulations is Z = 2.25. Combining our results for ϕ and Z thus highlights a universal adhesive regime characterized by the dimensionless parameter Ad. The resulting curve in the Z–ϕ plane, parametrized by Ad, can be considered as

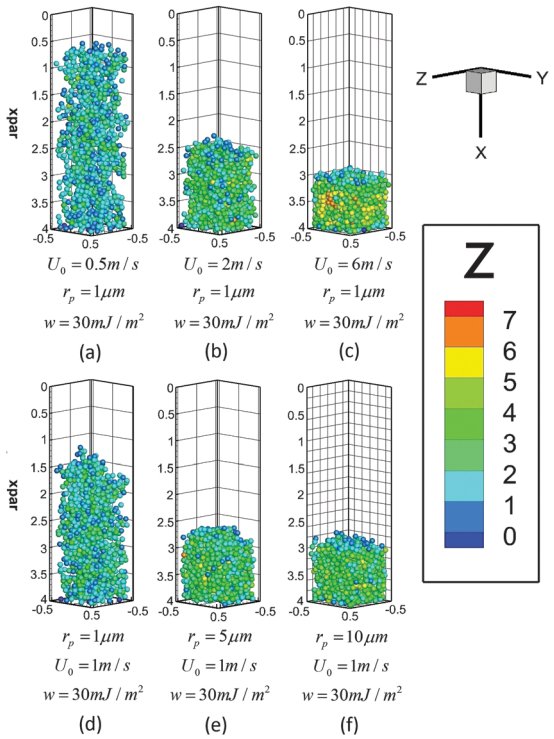

Fig. 1 Typical packing structure: different colors represent different coordination numbers Z. (a)–(c) Stand for U_0 = 0.5, 2 and 6 m s^{-1}, respectively, with particle radius r_p = 1 μm and work of adhesion w = 30 mJ m^{-2}. (d)–(f) Stand for r_p = 1, 5 and 10 μm, respectively, with U_0 = 1 m s^{-1} and w = 30 mJ m^{-2}.

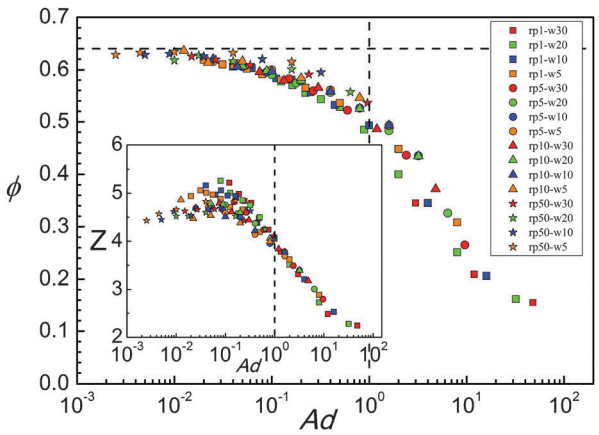

Fig. 2 Semi-log plot of the packing volume fraction as a function of adhesion parameter. $r_p1 - w30$ in the legend represents the particle radius r_p in units of μm and work of adhesion w in mJ m^{-2}. The horizontal red dash line indicates the limitation of ϕ_{RCP} = 0.64 and the vertical one the separation of Ad = 1. The inset shows the variation of the coordination number Z with Ad.

an equation of state of packings dominated by adhesion (see Fig. 4). It is worth noting that Z at Ad $\ll$ 1 does not reach the isostatic limit Z = 6 (of frictionless particles) even though the volume fraction approaches ϕ_{RCP} = 0.64. The reason is that we do not eliminate the effect of friction and all of our packings remain frictional with the friction coefficient μ_f = 0.3. Furthermore, the adhesion is so weak at Ad $\ll$ 1 that our simulation corresponds to adhesion-less frictional packings. As we decrease the friction at Ad $<$ 1, the curve in the Z–ϕ plane reaches RCP along the RLP–RCP line which is consistent with adhesion-less frictional packings (see the orange open triangles in Fig. 4).

Before we go on to the statistical theory of adhesive packings, it is important to examine the validity of our Ad scaling shown in Fig. 2. From the definition of Ad, we know that Ad reaches a critical value of Ad = 1 when the work of adhesion balances the particle inertia. With Ad $>$ 1 the adhesion dominates the packing, while it can be negligible when Ad $<$ 1. On the other hand, when Ad $<$ 1 the friction becomes more and more important so that our scaling may break down since Ad does not include friction. For instance, if the infinitely small Ad results from the sufficiently high particle velocity U_0, the packings approach the RCP limit because of the compression effect; if Ad and U_0 are both small implying a finite large particle radius, the friction-dependent RLP then applies.[17,19] Therefore it is assumed that the current theory works under the condition of Ad $>$ 1.

3 Statistical theory of packing with adhesion

We now derive an analytical representation of the adhesive equation of state in the spirit of Edwards' ensemble approach at the mean-field level.[6,11,44] We start with the Voronoi volume W_i of a reference particle i, which provides a tessellation of the total volume of the packing: $V = \sum_{i=1}^{N} W_i$. The key step is to use a statistical mechanical description, where we consider the average Voronoi volume $\overline{W} = \langle W_i \rangle$. This implies that $V = N\overline{W}$ and the packing fraction follows as $\phi = V_0/\overline{W}$. Here, V_0 is the volume of a sphere with radius r_p in the packing. In turn, $\overline{W}$ can be expressed exactly in terms of the pdf $p(c,Z)$ for finding the boundary of the Voronoi volume at a distance c from the sphere centre for a given z. We have[6,11]

$$\overline{W} = V_0 + 4\pi \int_{r_p}^{\infty} c^2 P(c,Z)\mathrm{d}c, \tag{4}$$

where $P(c,Z)$ is the CDF; $p(c,Z) = -\frac{\mathrm{d}}{\mathrm{d}c}P(c,Z)$. For $P(c,Z)$, one can derive a Boltzmann-like form using a factorization assumption of the multi-particle correlation function into pair correlations[44] to find

$$P(c,Z) = \exp\left\{-\rho \int_{\Omega(c)} \mathrm{d}\mathbf{r} g_2(\mathbf{r},Z)\right\}. \tag{5}$$

Here, $\rho = N/V = 1/\overline{W}$ is the number density and $g_2(\mathbf{r},Z)$ the pair correlation function of two spheres separated by $\mathbf{r}$. The volume $\Omega(c)$ is an excluded volume for the $N-1$ spheres outside of the reference sphere, since otherwise they would contribute a Voronoi boundary smaller than c. The exponential form eqn (5) is the key assumption in our mean-field approach, which corresponds to a minimal model of correlations motivated from high-dimensional sphere packings.[44] We then model the pair distribution function g_2 in terms of four distinct contributions following the results of

simulations and mean-field models of metastable glasses.[2,45–49] Indeed an important structure signature of jamming found in mean field replica models[2,45–50] is a power-law peak in the pair distribution function due to a large number of near contacting particles.[45–50] Quantitative bounds on the possible exponents of this power-law have been derived by imposing stability of the contact network under compression.[46,49] We consider: (1) a delta-peak due to contacting particles;[6,45,51] (2) a power-law peak over a range ε due to near contacting particles;[45,46] (3) a step function due to bulk particles;[6,51] and (4) a gap of width b separating the bulk and (near) contacting particles. This gap captures the effect of correlations due to adhesion and is assumed to depend on Z: $b = b(Z)$. In this way we model the increased porosity at a given Z compared with adhesion-less packings. Overall, we obtain

$$g_2(\mathbf{r}, Z) = \frac{Z}{\rho\lambda}\delta(r-2r_p) + \sigma(r-2r_p)^{-\nu}\Theta(2r_p+\varepsilon-r) + \Theta(r-(2r_p+b(Z))). \quad (6)$$

For the power law term, we assume $\nu = 0.38$ from[47] and a width of $\varepsilon = 0.1r_p$, which is approximately the range over which the peak decreases to the bulk value 1 as observed in ref. 45. The value σ is then fixed by continuity with the step function term in the absence of a gap. Next we have to determine the gap of width function $b(Z)$ which is the crucial assumption of the theory. $b(Z)$ needs to satisfy a set of constraints that we impose purely on physical grounds: (i) $b(Z)$ is a smooth monotonically decreasing function of Z. Here, the physical picture is that for small Z (corresponding to looser packings), the gap width is larger due to the increased porosity of the packing. (ii) At the isostatic limit $Z = 6$, the gap disappears, $b(6) = \varepsilon$, and we expect to recover the frictionless RCP value, since this value of Z represents a maximally dense disordered packing of spheres. We obtain from eqn (4)–(6) indeed the prediction of ref. 6 for RCP at $\phi_{Edw} = 0.634$ by choosing an appropriate value of λ. Moreover, we need to account for low dimensional corrections due to the hard-core excluded volume of the reference sphere, such that $\rho \to \bar{\rho} = 1/(\overline{W} - V_0)$, where V_0 is the volume of a sphere with radius r_p.[44] This constraint thus fixes ρ and λ, as well as one of the parameters in $b(Z)$. (iii) In addition, we conjecture the existence of an asymptotic adhesive loose packing (ALP) at $Z = 2$ and $\phi = 1/2^3$ which yields $b(2) = 1.47$ and fixes a second parameter in $b(Z)$. This is motivated by the fact that $\phi = 1/2^d$ is the well-known lower bound of saturated sphere packings in d dimensions.[51] Moreover, $Z = 2$ is the lowest possible value for a physical packing – if $Z < 2$, there are more spheres with a single contact (*i.e.*, dimers) than with three or more contacts, which identifies that the ALP point is only asymptotic.

Overall, we can thus in principle choose a parametric form of $b(Z)$ satisfying the above constraints. It is natural to use a three parametric form, *e.g.*, the exponential form $b(Z) = c_1 + c_2 e^{-c_3 Z}$ or a second order polynomial $b(Z) = c_1 + c_2 Z + c_3 Z^2$, such that one fitting parameter is left after the two constraints $b(6) = \varepsilon$ and $b(2) = 1.47$ are imposed. Or else just a simple linear form $b(Z) = c_1 + c_2 Z$ can be applied. Solving eqn (4)–(6) numerically for $\overline{W}$ (and thus ϕ) using the functional form of $b(Z)$ leads to a family of curves with a single free parameter, c_3. Fitting this parameter to the available data yields the value of c_3. Table 1 shows the fitting parameters of the three different forms of $b(Z)$ and Fig. 3 further highlights that the exponential decay of $b(Z)$ provides an excellent fit to the simulation data, while the linear or second order polynomial performs considerably worse. We then obtain a unique equation of state $\phi(Z)$ for adhesive packings as shown in Fig. 4 which agrees well with the simulation data. For large Ad values, the ALP point at (2, 0.125) is indeed approached in the Z–ϕ plane. The reduction of all the parameters in eqn (6) is then summarized in Table 2 for a clear expression. It should be noted that a direct fit of the continuation in the

Table 1 Fitting parameters of different forms of $b(Z)$

Forms	c_1	c_2	c_3
Exponential	$1.47/(1 - e^{4c_3})$	$1.47/(e^{-2c_3} - e^{-6c_3})$	1.0
Quadratic	$2.205 + 12c_3$	$-0.3675 - 8c_3$	0.09
Linear	2.205	−0.3675	

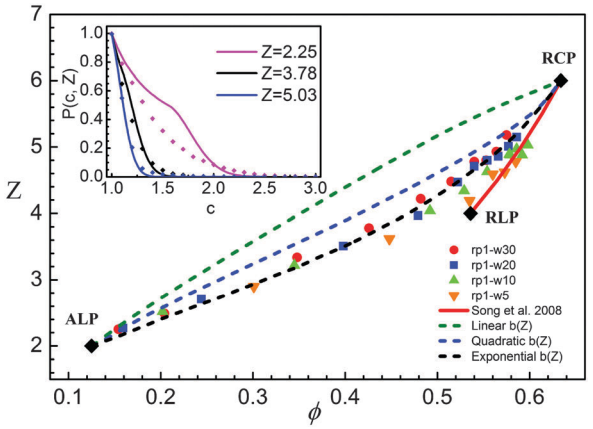

Fig. 3 Adhesion continuation with different forms of $b(Z)$. The inset shows a comparison of the theoretical $P(c,Z)$ (lines) under the exponential form of $b(Z)$ with the simulation data (dots).

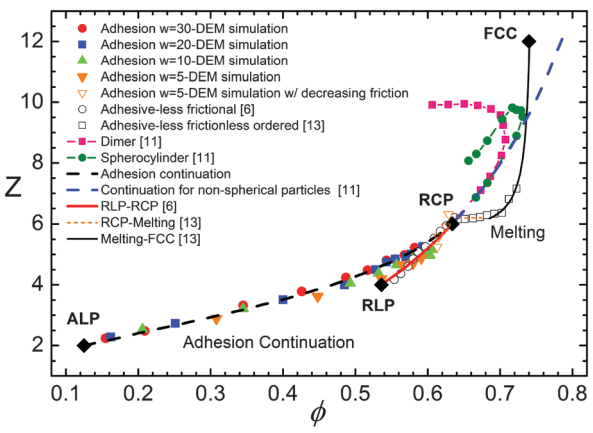

Fig. 4 Equation of state for adhesive packings: simulation data and theoretical prediction from eqn (4)–(6) with a single fitting parameter (black dashed line). The simulation data include only that of $r_p = 1$ μm in order to guarantee the typical adhesive characteristics of the packing.

Table 2 Summary of reduction of the fitting parameters

Parameters	Constraints	Values
ν	Assumption from ref. 47	0.38
ε	Assumption from ref. 45	$0.1r_p$
σ	Continuity with the step function term	Fixed value
ρ, λ	Isostatic limit $Z = 6$ from ref. 6	Fixed value
c_1	Isostatic limit $Z = 6$ from ref. 6	−0.0274
c_2	Asymptotic ALP conjecture and ref. 51	11.0646
c_3	Fitting parameter with the above parameters fixed	1.0

Z–ϕ plane with a second order polynomial would lead to similar results in the phase diagram. However, this would indeed be a fit without any physical insight contrary to our approach. As discussed above, we essentially have only a single free parameter to fit the continuation. Much more important though is the observation that the distribution of the Voronoi volumes $P(c,Z)$ (see the inset of Fig. 3) that results from our approach agrees well with the empirically observed distribution over the whole range of packing fractions observed, except for a "bump" in $P(c,Z)$ at low packing densities. It is an artifact of our theory which is caused by the sudden crossover from the δ-function term to the θ-function term in eqn (6). This means that including $b(Z)$ captures well the essential structural features of the packing. The fact that such a simple modification of the theory for non-adhesive particles, motivated on physical grounds, leads to such good agreement not only in the low density regime, but also for mid to high densities, is highly intriguing in our view.

4 Results and discussion

Including previous results from ref. 6, 11 and 13 in the Z–ϕ plane leads to a phase diagram of packings of frictionless, frictional, adhesive and adhesive-less spheres, as well as non-spherical particles (see Fig. 4). The collection of these results highlights the prominent role of the frictionless RCP point (ϕ_{Edw}) in the phase-diagram, despite that it contracts the J-line which has been corroborated in finite dimensional simulations with varying jamming protocols.[50,52,53] This jamming point ϕ_{Edw} is close to the lower boundary ϕ_{th} due to the large number of metastable glass states around ϕ_{th}. It is expected that the RSB J-line obtained for frictionless packings[2,7–9,50,52,53] would be an integral part of packings in general, loose and adhesion ones or perhaps even with friction as studied here. However, replica symmetry breaking packings are out of current reach of mathematical capabilities in these realistic cases. Thus such a J-point approximation could provide an effective perspective to look into the intrinsic physics of these numerous packings. From Fig. 4, we observe that non-spherical packings are smoothly continued at RCP into either the adhesive branch or the frictional branch. By contrast, the coexistence line from RCP to the melting point of crystalline packings, conjectured in ref. 13, does not connect smoothly to any of these branches. It suggests that particle deformation (which parametrizes the non-spherical branch) is a "natural" way to increase packing densities in disordered arrangements. On the other hand, introducing order is a more drastic modification, similar to a distinction between the discontinuous 1st and continuous higher-order phase transitions.

We now compare our athermal packings with gel phases in Brownian suspension, which exist over a similar range of densities.[33–37] By construction all our packings are percolating mechanically stable jammed packings with an infinite bond lifetime. Therefore, we identify the ALP as a minimal density packing for which a percolating contact network exists. By comparison, there exist indeed colloidal systems exhibiting a similar critical packing density ϕ_c dividing percolating and non-percolating aggregates in the $T \to 0$ limit.[32] When the liquid-gas phase separation is suppressed, *e.g.*, by long-range repulsion, a percolation threshold can be found at $\phi_c \approx 0.1$ for the $T \to 0$ separating cluster and network phases in a regime of large attraction strengths.[54–58] Alternatively, phase separation can be suppressed by artificially introducing an upper limit on the particle's coordination number, which shifts the spinodal decomposition to smaller T and ϕ. In this case, a percolating ideal gel phase is reached for $T \to 0$, where $\phi_c \approx 0.2$ separates the gel from the two-phase region.[59,60] Such an ideal gel also appears in a lattice model of attractive colloids, where $\phi_c \approx 0.1$.[61] Additionally, by decreasing the average short-ranged square well attraction sites per hard sphere patchy particles, disordered states can be reached at low T and very small $\phi_c(<0.13)$ without encountering phase separation.[62] In order to gain further structural insight we perform a topological cluster classification (TCC)[28,33] to characterize the structure. For small densities close to the ALP, we observe that (see Fig. 5) particles are mostly aggregated in clusters of m = 4, 5 and 3, indicating a tree-like packing structure with a coordination number of Z = 3. Here, m stands for the number of particles contained in a cluster. The low density cluster statistics is thus similar to models that impose an upper limit of Z.[59,60] For larger densities we can compare our packing structures with recent results on the TCC of gel and glass phases in a colloidal system of sticky spheres.[33] In this case, the major components

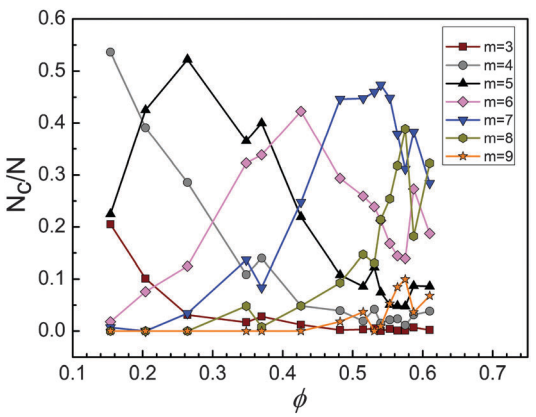

Fig. 5 Topological cluster classification of adhesive particle packings. The volume fraction is in the range of ϕ = 0.154–0.61 with Z = 2.25–5.18. m is the size of clusters and N_c/N stands for the fraction of clusters.

of our dense packing structure are clusters of m = 8, 7 and 6. Without any phase transition, our dense packing structures undergo a smooth change of dominating clusters from $m \approx 4$ to $m \approx 7$, which is quite different from the sudden changes in gel and glass transitions.[33]

5 Conclusions

In summary, we have identified a packing regime of adhesive small particles across 1 to 10^2 microns, using both DEM simulations and a statistical mechanical framework. Our results highlight that attraction in (spherical) particles leads to a lower density limit for percolation at the ALP with $\phi_c = 1/2^3$. The equivalent ϕ_c in attractive colloids is observed empirically over a range of densities $\phi_c \approx 0.1$–0.2 depending on the mechanism for the suppression of phase-separation. The situation is thus reminiscent of the adhesion-less and frictionless range of densities, $\phi \in [\phi_{th},\phi_{GCP}]$, predicted by mean field replica models.[2,7–9,50,52,53] As discussed in the Introduction our mean-field Edwards ensemble approach leads to a unique volume fraction ϕ_{Edw} which is extended along the adhesive line. It would be interesting to see if a similar range of jamming densities can be predicted for attractive interparticle forces. Replica approaches have indeed been applied to attractive colloids in high dimensions. Here, a reentrant glass transition and multiple glass states have been found.[63,64] More insight could be obtained by extending the full replica solution of jammed spheres in infinite dimensions[8,9] to incorporate both friction and adhesion, if possible.

Acknowledgements

This research was supported by NNSF of China (Nos. 51390491 and 50976058), NKBRDP (No. 2013CB228506), China AST, NSF-CMMT and Doe Geosciences Division. We thank J. Marshall, Q. Yao, G. Q. Liu, M. M. Yang, S. Chen, M. Denn, J. Morris, C. S. O'Hern, and E. Brown for discussions. AB acknowledges funding under EPSRC grant EP/L020955/1.

References

1 J. D. Bernal, *Nature*, 1959, **183**, 141–147.
2 G. Parisi and F. Zamponi, *Rev. Mod. Phys.*, 2010, **82**, 789–845.
3 S. Torquato and F. H. Stillinger, *Rev. Mod. Phys.*, 2010, **82**, 2633–2672.
4 M. van Hecke, *J. Phys.: Condens. Matter*, 2010, **22**, 033101.
5 C. S. O'Hern, L. E. Silbert, A. J. Liu and S. R. Nagel, *Phys. Rev. E: Stat., Nonlinear, Soft Matter Phys.*, 2003, **68**, 011306.
6 C. Song, P. Wang and H. A. Makse, *Nature*, 2008, **453**, 629–632.
7 R. Mari, F. Krzakala and J. Kurchan, *Phys. Rev. Lett.*, 2009, **103**, 025701.
8 P. Charbonneau, J. Kurchan, G. Parisi, P. Urbani and F. Zamponi, *Nat. Commun.*, 2014, **5**, 3725.
9 P. Charbonneau, J. Kurchan, G. Parisi, P. Urbani and F. Zamponi, *J. Stat. Mech.: Theory Exp.*, 2014, **2014**, P10009.
10 S. Edwards and R. Oakeshott, *Physica A*, 1989, **157**, 1080–1090.
11 A. Baule, R. Mari, L. Bo, L. Portal and H. A. Makse, *Nat. Commun.*, 2013, **4**, 2194.
12 A. Baule and H. A. Makse, *Soft Matter*, 2014, **10**, 4423–4429.
13 Y. Jin and H. A. Makse, *Phys. A*, 2010, **389**, 5362–5379.
14 M. P. Ciamarra and A. Coniglio, *Phys. Rev. Lett.*, 2008, **101**, 128001.
15 L. E. Silbert, *Soft Matter*, 2010, **6**, 2918–2924.
16 G. Y. Onoda and E. G. Liniger, *Phys. Rev. Lett.*, 1990, **64**, 2727–2730.
17 M. Jerkins, M. Schröter, H. L. Swinney, T. J. Senden, M. Saadatfar and T. Aste, *Phys. Rev. Lett.*, 2008, **101**, 018301.
18 K. J. Dong, R. Y. Yang, R. P. Zou and A. B. Yu, *Phys. Rev. Lett.*, 2006, **96**, 145505.
19 G. R. Farrell, K. M. Martini and N. Menon, *Soft Matter*, 2010, **6**, 2925–2930.
20 S. Li, J. S. Marshall, G. Liu and Q. Yao, *Prog. Energy Combust. Sci.*, 2011, **37**, 633–668.
21 J. S. Marshall and S. Li, *Adhesive Particle Flow*, Cambridge University Press, 2014.
22 C. Dominik and A. G. G. M. Tielens, *Astrophys. J.*, 1997, **480**, 647.
23 J. Blum and R. Schräpler, *Phys. Rev. Lett.*, 2004, **93**, 115503.
24 K. M. Kinch, J. Sohl-Dickstein, J. F. Bell, J. R. Johnson, W. Goetz and G. A. Landis, *J. Geophys. Res.: Planets*, 2007, **112**, E06S03.
25 R. Y. Yang, R. P. Zou and A. B. Yu, *Phys. Rev. E: Stat. Phys., Plasmas, Fluids, Relat. Interdiscip. Top.*, 2000, **62**, 3900–3908.
26 J. M. Valverde, M. A. S. Quintanilla and A. Castellanos, *Phys. Rev. Lett.*, 2004, **92**, 258303.
27 J. Blum, R. Schräpler, B. J. R. Davidsson and J. M. Trigo-Rodríguez, *Astrophys. J.*, 2006, **652**, 1768.
28 C. L. Martin and R. K. Bordia, *Phys. Rev. E: Stat., Nonlinear, Soft Matter Phys.*, 2008, **77**, 031307.
29 G. Lois, J. Blawzdziewicz and C. S. O'Hern, *Phys. Rev. Lett.*, 2008, **100**, 028001.
30 E. J. R. Parteli, J. Schmidt, C. Blumel, K.-E. Wirth, W. Peukert and T. Poschel, *Sci. Rep.*, 2014, **4**, 06227.
31 W. C. K. Poon, *J. Phys.: Condens. Matter*, 2002, **14**, R859.
32 E. Zaccarelli, *J. Phys.: Condens. Matter*, 2007, **19**, 323101.
33 C. P. Royall, S. R. Williams and H. Tanaka, *arXiv:cond-mat.soft/1409.5469*, 2014.
34 V. Trappe, V. Prasad, L. Cipelletti, P. N. Segre and D. A. Weitz, *Nature*, 2001, **411**, 772–775.
35 M. A. Miller and D. Frenkel, *Phys. Rev. Lett.*, 2003, **90**, 135702.
36 P. J. Lu, E. Zaccarelli, F. Ciulla, A. B. Schofield, F. Sciortino and D. A. Weitz, *Nature*, 2008, **453**, 499–503.
37 A. Fortini, E. Sanz and M. Dijkstra, *Phys. Rev. E: Stat., Nonlinear, Soft Matter Phys.*, 2008, **78**, 041402.
38 K. L. Johnson, K. Kendall and A. D. Roberts, *Proc. R. Soc. London, Ser. A*, 1971, **324**, 301–313.
39 M. Yang, S. Li and Q. Yao, *Powder Technol.*, 2013, **248**, 44–53.

40 L.-O. Heim, J. Blum, M. Preuss and H.-J. Butt, *Phys. Rev. Lett.*, 1999, **83**, 3328–3331.
41 J. Brujić, P. Wang, C. Song, D. L. Johnson, O. Sindt and H. A. Makse, *Phys. Rev. Lett.*, 2005, **95**, 128001.
42 H. A. Makse, J. Brujić and S. F. Edwards, *Statistical Mechanics of Jammed Matter*, Wiley-VCH Verlag GmbH & Co. KGaA, 2005, pp. 45–85.
43 S.-Q. Li and J. Marshall, *J. Aerosol Sci.*, 2007, **38**, 1031–1046.
44 Y. Jin, P. Charbonneau, S. Meyer, C. Song and F. Zamponi, *Phys. Rev. E: Stat., Nonlinear, Soft Matter Phys.*, 2010, **82**, 051126.
45 A. Donev, S. Torquato and F. H. Stillinger, *Phys. Rev. E: Stat., Nonlinear, Soft Matter Phys.*, 2005, **71**, 011105.
46 M. Wyart, *Phys. Rev. Lett.*, 2012, **109**, 125502.
47 E. Lerner, G. During and M. Wyart, *Soft Matter*, 2013, **9**, 8252–8263.
48 E. DeGiuli, E. Lerner, C. Brito and M. Wyart, *Proc. Natl. Acad. Sci. U. S. A.*, 2014, **111**, 17054–17059.
49 M. Müller and M. Wyart, *Annu. Rev. Condens. Matter Phys.*, 2015, **6**, 177–200.
50 P. Charbonneau, E. I. Corwin, G. Parisi and F. Zamponi, *Phys. Rev. Lett.*, 2012, **109**, 205501.
51 S. Torquato and F. H. Stillinger, *Experimental Mathematics*, 2006, **15**, 307–331.
52 M. Skoge, A. Donev, F. H. Stillinger and S. Torquato, *Phys. Rev. E: Stat., Nonlinear, Soft Matter Phys.*, 2006, **74**, 041127.
53 P. Chaudhuri, L. Berthier and S. Sastry, *Phys. Rev. Lett.*, 2010, **104**, 165701.
54 A. I. Campbell, V. J. Anderson, J. S. van Duijneveldt and P. Bartlett, *Phys. Rev. Lett.*, 2005, **94**, 208301.
55 R. Sanchez and P. Bartlett, *J. Phys.: Condens. Matter*, 2005, **17**, S3551.
56 F. Sciortino, P. Tartaglia and E. Zaccarelli, *J. Phys. Chem. B*, 2005, **109**, 21942–21953.
57 J. C. F. Toledano, F. Sciortino and E. Zaccarelli, *Soft Matter*, 2009, **5**, 2390–2398.
58 C. L. Klix, C. P. Royall and H. Tanaka, *Phys. Rev. Lett.*, 2010, **104**, 165702.
59 E. Zaccarelli, S. V. Buldyrev, E. La Nave, A. J. Moreno, I. Saika-Voivod, F. Sciortino and P. Tartaglia, *Phys. Rev. Lett.*, 2005, **94**, 218301.
60 E. Zaccarelli, I. Saika-Voivod, S. V. Buldyrev, A. J. Moreno, P. Tartaglia and F. Sciortino, *J. Chem. Phys.*, 2006, **124**, 124908.
61 F. Krzakala, M. Tarzia and L. Zdeborová, *Phys. Rev. Lett.*, 2008, **101**, 165702.
62 E. Bianchi, J. Largo, P. Tartaglia, E. Zaccarelli and F. Sciortino, *Phys. Rev. Lett.*, 2006, **97**, 168301.
63 M. Sellitto and F. Zamponi, *J. Phys.: Conf. Ser.*, 2013, **473**, 012020.
64 M. Sellitto and F. Zamponi, *EPL*, 2013, **103**, 46005.

